ELSEVIER

Contents lists available at ScienceDirect

## Electric Power Systems Research

journal homepage: www.elsevier.com/locate/epsr





## Estimation of lightning channel-base current from far electromagnetic field in the case of inclined channel

K. Kutsuna <sup>a,\*</sup>, N. Nagaoka <sup>a</sup>, Y. Baba <sup>a</sup>, T. Tsuboi <sup>b</sup>, V.A. Rakov <sup>c</sup>

- <sup>a</sup> Doshisha University, Department of Electrical Engineering, Kyoto 610-0394, Japan
- <sup>b</sup> TEPCO Research Institute, Yokohama, Kanagawa 230-8510, Japan
- <sup>c</sup> University of Florida, Department of Electrical and Computer Engineering, Gainesville FL 32611, USA

## ARTICLE INFO

# Keywords: Lightning Lightning return stroke Inclined lightning channel Lightning current Lightning electromagnetic field Inverse problem

## ABSTRACT

The inclination of a lightning return-stroke channel significantly affects the waveform of the associated electromagnetic field. In this paper, we have derived mathematical expressions to estimate the peak and waveshape of lightning return-stroke current at the channel base from the waveform of electromagnetic field observed more than some tens of kilometers away from an inclined lightning channel. Three models of the lightning return stroke are considered, which are the transmission-line (TL) model, the modified TL model with linear current decay with height (MTLL), the modified TL model with exponential current decay with height (MTLE). The peak of the lightning return-stroke current at the channel base is estimated from the peak of observed lightning electric or magnetic field using an analytical relation between the peak of channel-base current and that of the radiation field component for an inclined channel. The waveform of the channel-base current is reconstructed from the electric or magnetic field waveform using a relation between the channel-base current and the sum of induction and radiation field components for an inclined channel. It has been shown that the peak and waveshape of current at the base of an inclined channel are sufficiently accurately estimated with the proposed expressions. This work is the first attempt to solve the inverse problem (infer source parameters from electromagnetic fields) for the case of inclined lightning channel. Solving this problem is important for developing methodology of remote measurements of lightning currents.

## 1. Introduction

All processes comprising a lightning discharge are associated with the motion of electric charges and, hence, produce electric and magnetic fields. By measuring these fields one can estimate various lightning parameters, such as electric current, charge transfer, etc. (see, for example, Kodali et al. (2005) [1] and Qie et al. (2009) [2]), needed in different areas of lightning research and protection. There have been many attempts to infer lightning return stroke currents from remotely measured (essentially radiation) electric and magnetic fields (e.g., Norinder and Dahle (1945) [3]; Uman and McLain (1970) [4]; Uman et al. 1973 [5,6]; Dulzon and Rakov (1980) [7]; Krider et al. (1996) [8]; Cummins et al. (1998) [9]; Rachidi et al. (2004) [10]; Mallick et al. (2014) [11]). Such "remote" measurements are model dependent and, therefore, inferior to direct measurements. However, they remain attractive because they allow one to acquire a large (statistically significant) sample over a relatively short period of time for lightning

events that are not influenced by tall strike objects that are usually required for direct measurements.

Rachidi and Thottappillil (1993) [12] have reviewed expressions relating vertical electric fields at far distances on perfectly conducting ground to channel-base currents for several engineering models of lightning return stroke. The waveform of channel-base current is given by the time integration of the far field for the model proposed by Bruce and Golde (1941) [13]. The channel-base-current waveform is simply proportional to that of the far field for the transmission-line (TL) model (Uman and McLain 1969) [14]. It is the solution of a first-order differential equation for the modified TL model with exponential current decay with height (MTLE) (Nucci et al. 1988) [15] or the model proposed by Master et al. (1981) [16]. The channel-base current is given as the series of the time-shifted far field for the traveling-current-source model (Heidler 1985) [17], and as the series of the sum of the time-shifted far field and its time derivative for the model proposed by Diendorfer and Uman (DU) [18]. In each of these conversion equations

E-mail address: ctwf0328@gmail.com (K. Kutsuna).

<sup>\*</sup> Corresponding author.

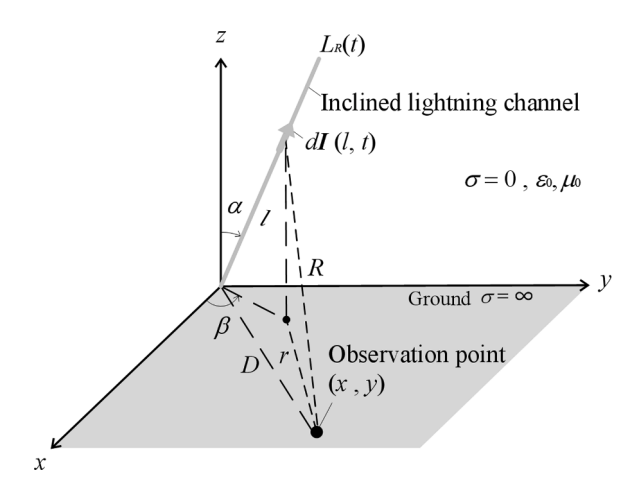


Fig. 1. Geometry of inclined lightning channel and postion of observation point on perfectly conducting ground.

from the far-field waveform to its causative channel-base-current waveform, all the values of the return-stroke-model parameters, such as the return-stroke speed used in far-field computations, are needed.

For the MTLE model and the modified TL model with linear current decay with height (MTLL) (Rakov and Dulzon 1987) [19], Andreotti et al. (2000) [20] have developed two different procedures to estimate the height-dependent attenuation factor in the frequency domain, when the return-stroke propagation speed, the channel-base current, and the vertical electric field on perfectly conducting ground are given. In one procedure, the vertical electric field at different frequencies (ranging from 50 Hz to 1 MHz) at one distance (0.5 km) from the lightning channel is used. In the other procedure, vertical electric fields calculated at one frequency (1 MHz) at different distances (ranging from 50 m to 2 km) from the channel are employed. They have demonstrated that the height-dependent attenuation factors are estimated reasonably accurately with either of these two procedures.

Popov et al. (2000) [21] have proposed two procedures to obtain the waveform of channel-base current along with the parameters of the DU model, which are the discharge time constant, the upward return-stroke front speed, and the downward current-wave propagation speed from two-station field measurements: (a) azimuthal magnetic fields at intermediate and near distances or (b) vertical electric or azimuthal magnetic field at far and near distances. An explicit inversion expression using the induction and radiation components of the azimuthal magnetic field was derived.

Recently, Fukuyama et al. (2021) [22] have derived expressions for reconstructing the waveform of channel-base current in a recurrence-relation form from the waveform of vertical electric field on perfectly conducting ground at a far distance for the MTLL and MTLE models. Also, they have shown that the waveforms of channel-base current are reconstructed well using the proposed expressions from the waveforms of vertical electric field.

El Dein et al. (2014) [23] and Abouzeid et al. (2015) [24] have derived expressions of electric and magnetic fields produced by a current propagating upward along an inclined lightning return-stroke channel. However, there are no expressions in the existing literature for reconstructing the waveform of channel-base current from the waveform of electric or magnetic field produced by an inclined lightning channel.

Lightning electromagnetic fields for the case of inclined channels were considered, mostly in the context of evaluation of voltages induced on horizontal conductors by Sakakibara (1989) [25], Michishita et al.

(1996) [26], Moini et al. (2006) [27], Matsubara and Sekioka (2009) [28], and Andreotti et al. (2012) [29], among others. Recently, currents in the shield conductor of buried coaxial cable induced by inclined lightning return-stroke channels were studied by Foroughi Nematollahi and Vahidi (2022) [30].

In this paper, mathematical expressions to estimate the peak and waveshape of lightning return-stroke current at the channel base from the waveform of electric or magnetic field observed more than some tens of kilometers away from an inclined lightning channel are derived. Three engineering models of the lightning return stroke, which are the TL model, the MTLL model, and the MTLE model, are employed. This paper is organized as follows, In Section 2, an expression for the vertical electric field on a perfectly conducting ground associated with a current propagating upward along an inclined lightning channel is given. Also, expressions for the current along the channel specified by the three return-stroke models are presented. In Section 3, waveforms of vertical electric field at a distance of 100 km from the base of inclined channel computed for these return-stroke models are shown. In Section 4, an expression to estimate the peak of current at the base of inclined channel from the peak of vertical electric field is derived. In Section 5, an expression to reconstruct the entire waveform of current at the base of inclined channel in a recurrence-relation form from the waveform of vertical electric field on perfectly conducting ground is derived. Also, the validity of the proposed current-reconstruction expression is demonstrated. In the Appendix, expressions to estimate the peak and the overall shape of lightning return-stroke current waveform at the channel base from the waveform of azimuthal magnetic field observed more than some tens of kilometers away from an inclined lightning channel are presented, and their validity is tested. The results will be useful in developing practical tools for solving the non-trivial inverse problem of finding source parameters from measured lightning electromagnetic fields.

## 2. Mathematical expressions of vertical electric field produced by an inclined lightning channel represented by engineering return-stroke models

# 2.1. General expression of vertical electric field produced by an inclined lightning channel

The vertical electric field  $E_z$  at the observation point (x, y) on a perfectly conducting ground associated with a current wave I

propagating along an inclined lightning channel, as shown in Fig. 1, derived by El Dein et al. (2014) [23] and Abouzeid et al. (2015) [24], is given as follows:

$$E_{z}(x, y, t) = E_{zs} + E_{zi} + E_{zr}$$

$$= \int_{0}^{L_{R}(t)} C_{ezs}(l) \int_{0}^{t} I(l, \tau - R/c) d\tau dl$$

$$+ \int_{0}^{L_{R}(t)} C_{ezi}(l) I(l, t - R/c) dl$$

$$- \int_{0}^{L_{R}(t)} C_{ezr}(l) \frac{\partial I(l, t - R/c)}{\partial t} dl$$
(1)

where

$$C_{ezs}(l) = \frac{(3z'2 - R^2)\cos\alpha - 3z'\sin\alpha[(x - x')\cos\beta + (y - y')\sin\beta]}{2\pi\varepsilon_0 R^5}$$

$$C_{ezi}(l) = \frac{(3z'^2 - R^2)\cos\alpha - 3z'\sin\alpha[(x - x')\cos\beta + (y - y')\sin\beta]}{2\pi\varepsilon_0 cR^4}$$

$$C_{ezi}(l) = \frac{z'\sin\alpha[((x - x')\cos\beta + (y - y')\sin\beta)] + r^2\cos\alpha}{2\pi\varepsilon_0 c^2 R^3}$$

$$l = \sqrt{x'2 + y'2 + z'2}$$

$$R = \sqrt{(x - x')^2 + (y - y')^2 + z^2}$$

$$= \sqrt{(x - l\sin\alpha\cos\beta)^2 + (y - l\sin\alpha\sin\beta)^2 + (l\cos\alpha)^2}$$

$$= \sqrt{x^2 + y^2 - 2xl\sin\alpha\cos\beta - 2yl\sin\alpha\sin\beta + l^2}$$

$$= \sqrt{x^2 + y^2 - 2l\sin\alpha(x\cos\beta + y\sin\beta) + l^2}$$

$$= \sqrt{D^2 - 2l\sin\alpha(x\cos\beta + y\sin\beta) + l^2}$$

$$D = \sqrt{x^2 + y^2}$$

$$r = \sqrt{(x - x')^2 + (y - y')^2}$$

where  $\varepsilon_0$  is the permittivity of vacuum, c is the speed of light, and v is the current propagation speed along the inclined channel. The lightning channel is tilted from the z axis with angle  $\alpha$  and from the x axis with angle  $\beta$ . Point (x', y', z') is the location of infinitesimal current element dI.  $L_R(t)$  is the radiating channel length (see, for example, Fig. 19 in [34]); that is, the length of the lightning channel within which the current elements contribute to the field at the observation point at time t. It is given by the solution of the following equation:  $t = L_R(t)/v + R$   $(L_R(t))/c$ . The first, second, and third terms of Eq. (1) are referred to as electrostatic  $E_{zs}$ , induction  $E_{zi}$  and radiation  $E_{zr}$  components, respectively.

## 2.2. Engineering models of lightning return stroke

Three engineering models, the TL, MTLL, and MTLE models are considered in this paper. In each of these models, the relation between the current at the distance l along the channel from it's base at time t and the current at the channel base, l = 0, is given as follows:

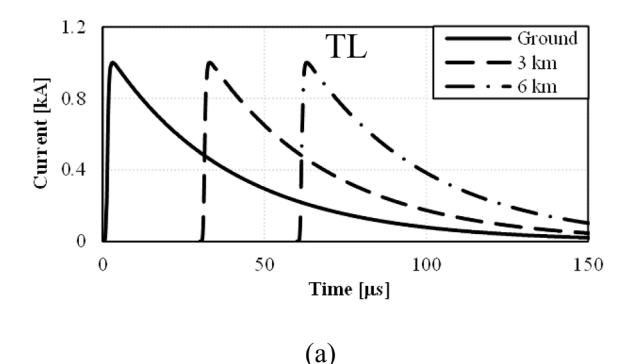
$$I(l, t) = I(0, t - l/\nu)$$
(3)

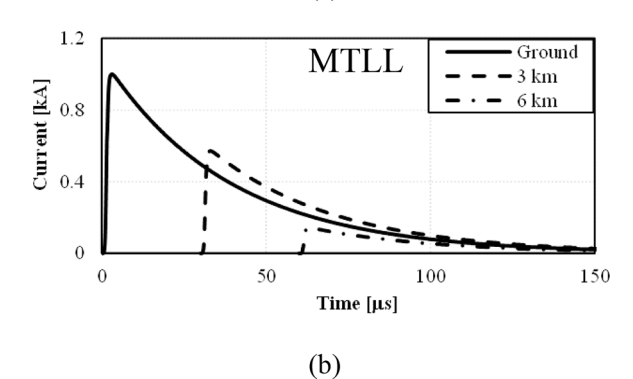
$$I(l, t) = (1 - l/L)I(0, t - l/v)$$
(4)

$$I(l, t) = \exp(-l/\lambda)I(0, t - l/\nu)$$
(5)

where L is the total length of the lightning channel, and  $\lambda$  is the current decay constant of the MTLE model.

Fig. 2 shows waveforms of lightning current at three different points,





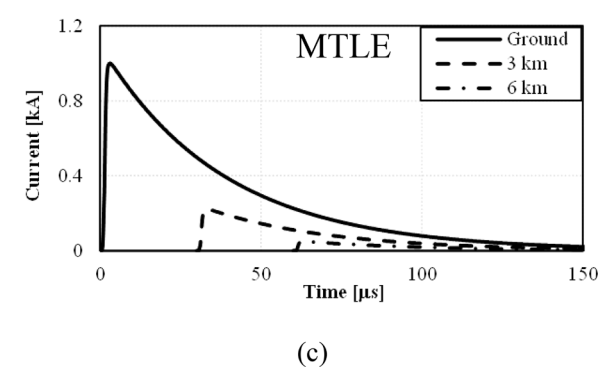


**Fig. 2.** Waveforms of lightning current at three different points, l=0 (on the ground), 3, and 6 km along the channel from the channel base computed with (a) the TL model (Eq. (3), (b) the MTLL model Eq. (4), and (c) the MTLE model Eq. (5). Note that L=7 km,  $\lambda=2$  km, and  $\nu=c/3$ .

l=0 (on the ground), 3, and 6 km along the channel from the channel base computed with the TL, MTLL, and MTLE models. The total length of the lightning channel is set to L=7 km current propagation speed is set to v=c/3 (Rakov 2007 [31]) in the models. The current decay constant in the all MTLE model is set to  $\lambda=2$  km. The waveform of channel-base current is represented by the Heidler function, which is given as follows (Heidler 1985 [32]):

$$I(t) = I_0 \frac{(t/\tau_1)^6}{1 + (t/\tau_1)^6} \exp(-t/\tau_2)$$
(6)

where  $I_0=1.1$  kA,  $\tau_1=1.5$   $\mu s$  and  $\tau_2=38$   $\mu s$ . The peak of the current waveform is 1 kA. The risetime and half-peak width are 1  $\mu s$  and 30  $\mu s$ , respectively.

## 2.3. Modeling configuration

Fig. 3 shows the configuration of the inclined lightning channel and the field observation point in the y–z plane ( $\beta = 90^{\circ}$  in Fig. 1). The

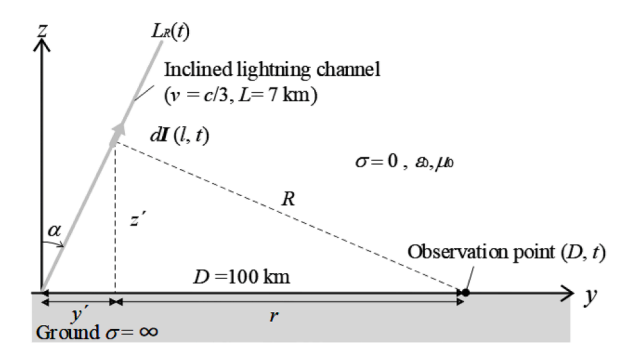


**Fig. 3.** Configuration of the inclined lightning channel and the field observation point on the y–z plane ( $\beta$  = 90° in Fig. 1). The channel inclination angle  $\alpha$  from the z axis is set to a value ranging from -60 to +60°, where the positive angle indicates the channel tiltle to the observation point. The distance between the channel base and the observation point is D = 100 km.

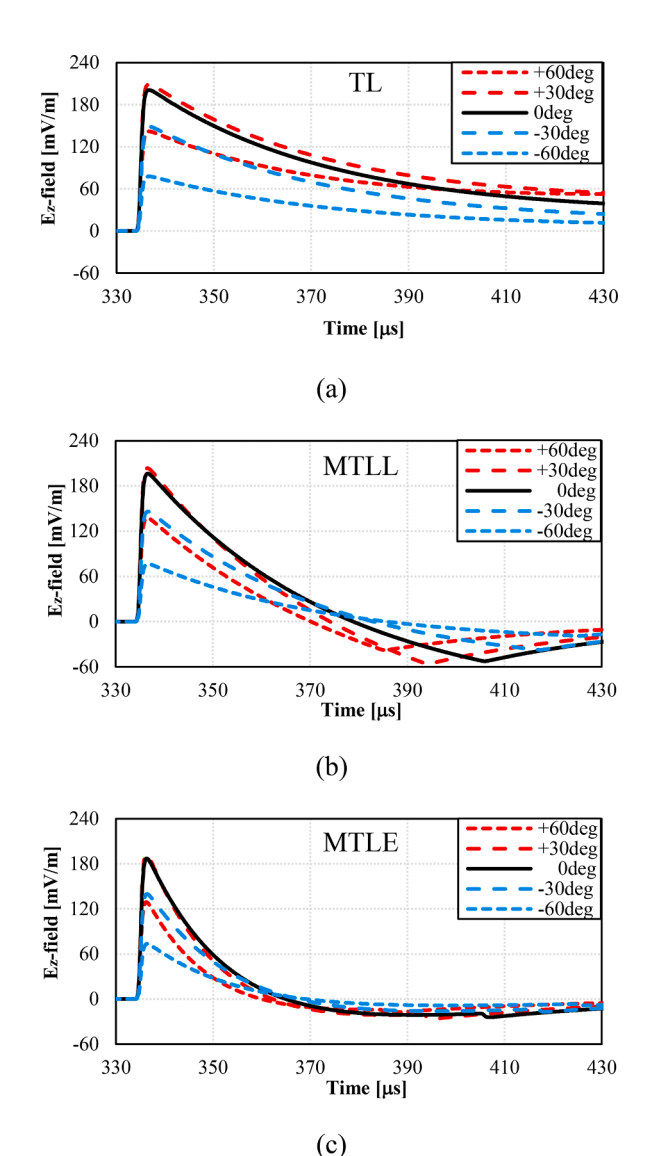


**Fig. 4.** Vertical electric field waveforms for unit-peak channel-base current waveform at a distance of 100 km from the base of an inclined lightning channel computed with (a) the TL model, (b) the MTLL model, and (c) the MTLE model (see Fig. 2) for different inclination angles:  $\alpha = -60$ , -30, 0, +30 and +60 deg. ( $RT = 1 \mu s$ ,  $\nu = c/3$ ).

Table 1
Peaks of vertical electric field waveforms for 1-kA-peak current waveforms shown in Fig. 2 at a distance of 100 km from the base of the inclined lightning channel. Units [mV/m].

| Model | Inclination angle of lightning channel $\alpha$ |         |       |         |         |  |
|-------|---|---------|-------|---------|---------|--|
|       | -60 deg   | -30 deg | 0 deg | +30 deg | +60 deg |  |
| TL    | 77.8  | 149     | 201   | 209     | 142     |  |
| MTLL  | 76.4  | 146     | 196   | 204     | 137     |  |
| MTLE  | 73.5  | 140     | 187   | 193     | 129     |  |

channel inclination angle  $\alpha$  from the z axis is set to a value ranging from -60 to +60° (the practical range is probably from -45 to +45°), where the positive angle indicates the channel tilted to the observation point. The distance between the channel base and the observation point is D=100 km. The reason why D=100 km is employed here is that this distance has been frequently selected in comparison of far electromagnetic field waveforms computed with "engineering" return-stroke models (field e.g., Nucci et al. 1990 [33]; Rakov and Uman 1998 [34]).

## 3. Computed vertical electric field waveforms

Fig. 4 shows waveforms of the vertical electric field at a distance of 100 km from the base of an inclined lightning channel computed with the TL, MTLL, and MTLE models, for different inclination angles,  $\alpha = -60$ , -30, 0 (vertical channel), +30 and +60°. Table 1 gives the peaks of the vertical electric field.

It appears from Fig. 4 and Table 1 that vertical electric fields at  $D=100\,\mathrm{km}$  are influenced significantly by the channel inclination. Therefore, it is desirable to consider the channel inclination when the peak and overall waveform of channel-base current are estimated or reconstructed from the waveform of vertical electric field. Note that the waveshapes of vertical electric field computed with the MTLL and MTLE models shown in Figs. 4(b) and (c) are different from that of the channel-base current, while the waveshape of the vertical electric field computed with the TL model shown in Fig. 4(a) is the same as that of the channel-base current. The channel-base current is the same for all three models and is shown by solid line in Fig. 2. Also note that almost the same electric-field peaks are yielded by the TL, MTLL, and MTLE models.

## 4. Expression for estimating the peak of the lightning channel-base current

In this section, we derive an expression to estimate the current peak at the lightning channel base from the electric-field peak considering the inclination of lightning channel. The initial peak of lightning electric or magnetic field waveform beyond some tens of kilometers is essentially due to its radiation component. The radiation component of the vertical electric field, which is the third term of the right-hand side of Eq. (1), is rewritten as follows:

$$E_z(x, y, t) \approx E_{zr}(x, y, t) = -\int_0^{L_R(t)} C_{exr}(t) P(t) \frac{\partial I(t - R/c - l/v)}{\partial t} dt$$
 (7)

where P(l) is the current attenuation function, which is different for the three models considered here (see Eqs. (3) to (5))

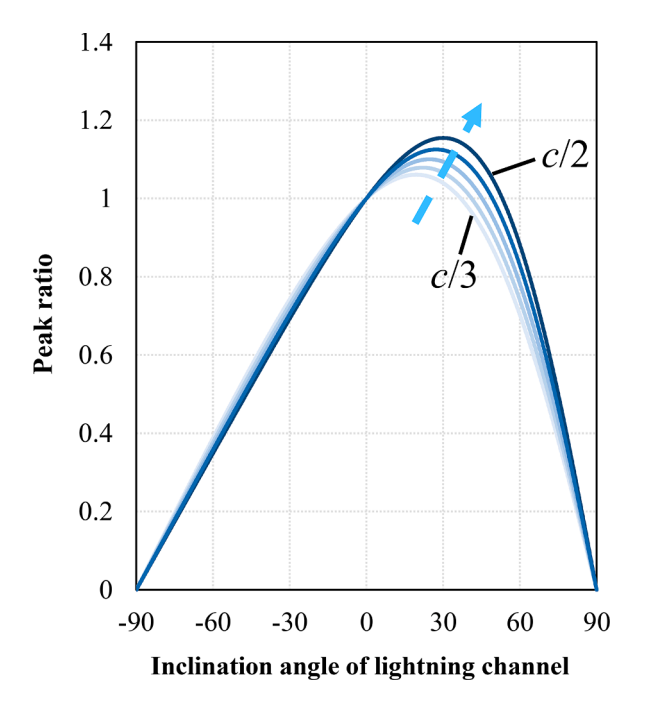
The partial time derivative in Eq. (7) is replaced by the partial spatial derivative in terms of l as follows:

**Table 2**Channel-base-current peaks estimated from far vertical electric-field peaks without considering channel inclination. The actual current peak is 1 kA.

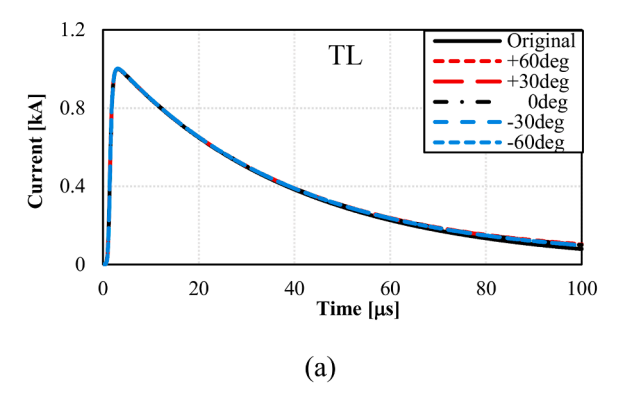
| Model | Inclination | Inclination angle of lightning channel $\alpha$ |       |         |         |  |  |
|-------|-------------|---|-------|---------|---------|--|--|
|       | -60 deg     | -30 deg   | 0 deg | +30 deg | +60 deg |  |  |
| TL    | 0.39        | 0.75  | 1.0   | 1.0     | 0.71    |  |  |
| MTLL  | 0.38        | 0.73  | 0.98  | 1.0     | 0.69    |  |  |
| MTLE  | 0.37        | 0.70  | 0.94  | 0.96    | 0.65    |  |  |

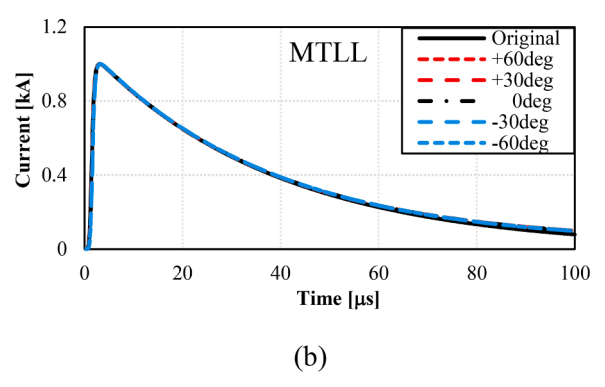
 $\begin{tabular}{ll} \textbf{Table 3} \\ \textbf{Channel-base-current peaks estimated from far vertical electric-field peaks} \\ \textbf{considering channel inclination. The actual current peak is 1 kA.} \\ \end{tabular}$ 

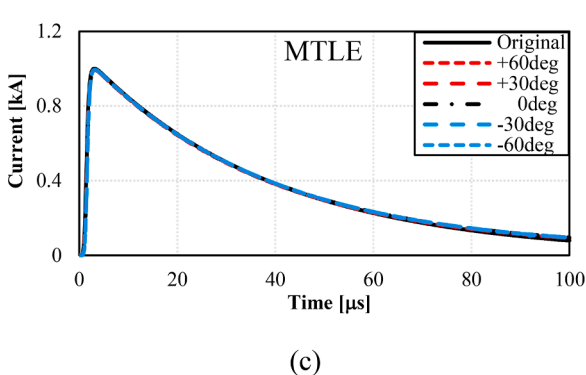
| Model | Inclination angle of lightning channel $\alpha$ |         |       |         |         |  |
|-------|---|---------|-------|---------|---------|--|
|       | -60 deg   | -30 deg | 0 deg | +30 deg | +60 deg |  |
| TL    | 1.0   | 1.0     | 1.0   | 1.0     | 1.0     |  |
| MTLL  | 0.99  | 0.98    | 0.98  | 0.98    | 0.98    |  |
| MTLE  | 0.95  | 0.94    | 0.94  | 0.93    | 0.92    |  |



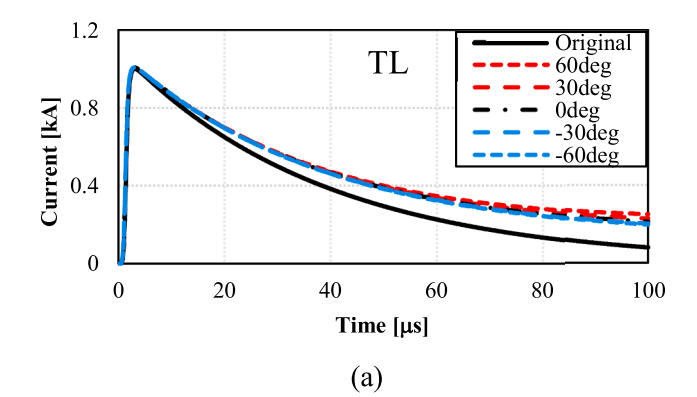
**Fig. 5.** Ratio of the electric-field peak at a distance of 100 km from the channel base, in the case of a channel with an angle  $\alpha$  (when  $\beta=90^\circ$ ) ranging from -90 to  $90^\circ$  (the limiting angle values are included just for completeness), to the electric-field peak in the case of vertical channel ( $\theta=0$ ), calculated using Eq. (12). The propagation speed of lightning return-stroke current is set to a vary from c/3 to c/2.

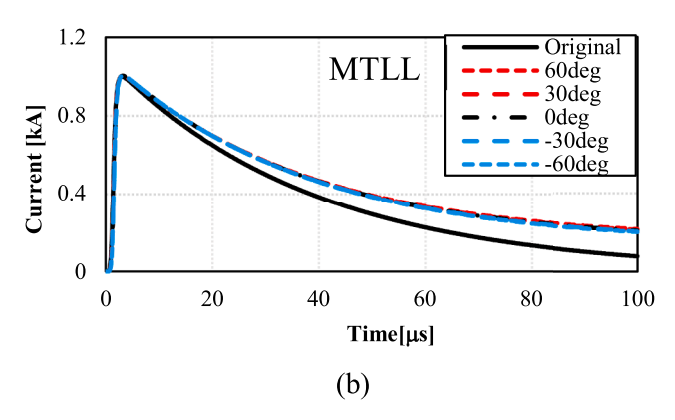






**Fig. 6.** Waveforms of channel-base current estimated from vertical electric-field waveforms (both induction and radiation field components are taken into account) at a distance of 100 km from the inclined lightning channel with (a) the TL model, (b) the MTLL model, and (c) the MTLE model for different inclination angles:  $\alpha=$ -60, -30, 0, +30 and +60 deg ( $RT=1~\mu s, \nu=c/3$ ). Additionally shown by solid black line is the original channel-base current waveform, which is indistinguishable from the current waveforms estimated from field waveforms. Relatively small differences in the tail (at 100  $\mu s$ ) are quantified in Table 4.





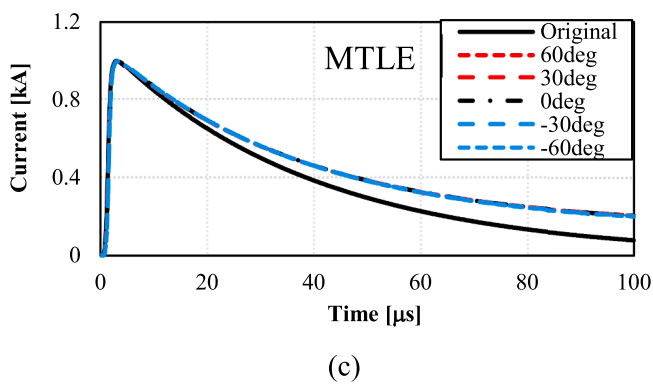


Fig. 7. Same as Fig. 6, but neglecting the induction field component. Note appreciable differences between the original and estimated current waveforms at later times, quantified at  $100~\mu s$  in Table 5.

Table 4 Ratio of the channel-base current at 100  $\mu$ s estimated with Eq. (17) to the corresponding original value.

| Model | Inclination | Inclination angle of lightning channel $\alpha$ |       |         |         |  |  |
|-------|-------------|---|-------|---------|---------|--|--|
|       | -60 deg     | -30 deg   | 0 deg | +30 deg | +60 deg |  |  |
| TL    | 1.2         | 1.3   | 1.3   | 1.3     | 1.3     |  |  |
| MTLL  | 1.2         | 1.2   | 1.2   | 1.2     | 1.2     |  |  |
| MTLE  | 1.2         | 1.2   | 1.2   | 1.2     | 1.2     |  |  |

Table 5
Ratio of the channel-base current at 100 μs estimated with an equation neglecting the induction component to the corresponding original value.

| Model | Inclination | Inclination angle of lightning channel $\alpha$ |       |         |         |  |  |
|-------|-------------|---|-------|---------|---------|--|--|
|       | -60 deg     | -30 deg   | 0 deg | +30 deg | +60 deg |  |  |
| TL    | 1.5         | 1.6   | 1.7   | 1.9     | 2.2     |  |  |
| MTLL  | 1.6         | 1.6   | 1.7   | 1.7     | 1.8     |  |  |
| MTLE  | 1.5         | 1.6   | 1.6   | 1.6     | 1.6     |  |  |

$$\begin{cases}
I = t - R/c - l/v \\
\frac{\partial I(t - R/c - l/v)}{\partial t} = \frac{\partial I(T)}{\partial t} = \frac{\partial I(T)}{\partial T} \frac{\partial T}{\partial t} = \frac{\partial I(T)}{\partial T} = \frac{\partial I(t - R/c - l/v)}{\partial T} \\
\frac{\partial I(t - R/c - l/v)}{\partial l} = \frac{\partial I(T)}{\partial l} = \frac{\partial I(T)}{\partial T} \frac{\partial T}{\partial l} \\
= \left[ \frac{\sin\alpha(x\cos\beta + y\sin\beta) - l}{c\sqrt{D^2 - 2l\sin\alpha(x\cos\beta + y\sin\beta) + l^2}} - \frac{1}{v} \right] \frac{\partial I(T)}{\partial T} \\
= \left[ \frac{\sin\alpha(x\cos\beta + y\sin\beta) - l}{c\sqrt{D^2 - 2l\sin\alpha(x\cos\beta + y\sin\beta) + l^2}} - \frac{1}{v} \right] \frac{\partial I(t - R/c - l/v)}{\partial t} \\
\text{or, in compact form,} \\
\frac{\partial I(t - R/c - l/v)}{\partial t} = S(l) \frac{\partial I(t - R/c - l/v)}{\partial l} \\
\text{where } S(l) = \frac{1}{\sin\alpha(x\cos\beta + y\sin\beta) - l} - \frac{1}{v} \end{aligned}$$

Note that in evaluating  $\partial \Gamma/\partial l$  in (8) we used

$$\frac{\partial R}{\partial l} = \frac{-2\sin\alpha(x\cos\beta + y\sin\beta) + 2l}{2\sqrt{D^2 - 2l\sin\alpha(x\cos\beta + y\sin\beta) + l^2}}$$
$$= \frac{-\sin\alpha(x\cos\beta + y\sin\beta) + l}{\sqrt{D^2 - 2l\sin\alpha(x\cos\beta + y\sin\beta) + l^2}}$$

Substitution of Eq. (8) into Eq. (7) yields

$$\begin{split} E_z(x,\ y,\ t) &\approx -\int_0^{L_R(t)} C_{ezr}(t) P(t) S(t) \frac{\partial I(t-R/c-l/v)}{\partial l} dl \\ &= -C_{ezr}(t) P(t) S(t) I(t-R/c-l/v)|_{l=0}^{l=L_R(t)} \\ &+ \int_0^{L_R(t)} \frac{\partial}{\partial l} [C_{ezr}(t) P(t) S(t)] I(t-R/c-l/v) dl \\ &= -C_{ezr}(L_R(t)) P(L_R(t)) S(L_R(t)) I(t-R/c-L_R(t)/v) \\ &+ C_{ezr}(0) P(0) S(0) I(t-D/c) \\ &+ \int_0^{L_R(t)} \frac{\partial}{\partial l} [C_{ezr}(t) P(t) S(t)] I(t-R/c-l/v) dl \\ \end{split}$$
 where  $C_{ezr}(0) = \frac{D^2 \cos \alpha}{2\pi \varepsilon_0 c^2 D^3} = \frac{\cos \alpha}{2\pi \varepsilon_0 c^2 D}$  
$$P(0) = 1$$
 
$$S(0) = \frac{vcD}{v \sin \alpha (x \cos \beta + y \sin \beta) - cD}$$

Therefore

$$E_{z}(x, y, t) = -C_{ezr}(L_{R}(t))P(L_{R}(t))S(L_{R}(t))I(t - R/c - L_{R}(t)/v)$$

$$+ \frac{\cos\alpha}{2\pi\epsilon_{0}c^{2}D} \frac{vcD}{v\sin\alpha(x\cos\beta + y\sin\beta) - cD}I(t - D/c)$$

$$+ \int_{0}^{L_{R}(t)} \frac{\partial}{\partial l}[C_{ezr}(l)P(l)S(l)]I(t - R/c - l/v)dl$$

$$= -C_{ezr}(L_{R}(t))P(L_{R}(t))S(L_{R}(t))I(t - R/c - L_{R}(t)/v)$$

$$- \frac{\mu_{0}cv\cos\alpha}{2\pi[cD - v\sin\alpha(x\cos\beta + y\sin\beta)]}I(t - D/c)$$

$$+ \int_{0}^{L_{R}(t)} \frac{\partial}{\partial l}[C_{ezr}(l)P(l)S(l)]I(t - R/c - l/v)dl$$
(10)

Since the first term is zero and the contribution of the second term is expected to be negligibly small in comparison with that of the first term around the time of the initial peak, the vertical electric field around the time of the initial peak is approximated as follows:

$$E_z(x, y, t) \approx -\frac{\mu_0 c v \cos \alpha}{2\pi [cD - v \sin \alpha (x \cos \beta + y \sin \beta)]} I(t - D/c)$$
 (11)

Therefore, the channel-base current peak  $I_{peak}$  is estimated from the peak of the vertical electric field  $E_{zpeak}$  at a far distance as follows:

$$I_{peak} \approx k_{ez} E_{zpeak}$$

$$k_{ez} = \frac{2\pi [cD - v\sin\alpha(x\cos\beta + y\sin\beta)]}{\mu_0 cv\cos\alpha}$$
(12)

where  $k_{ez}$  is an electric-field-to-current conversion factor. Note that angles  $\alpha$  and  $\beta$  in Eq. (12) needed to estimate the current peak can be obtained on the basis of optical observations of lightning channel from two different directions (e.g., Hubert and Mouget 1981 [35]; Idone et al. 1984 [36]; Willett et al. 2008 [37]; Lu et al. 2015 [38]). For a vertical lightning channel ( $\alpha$ = 0),  $k_{ez}$  is given simply as follows:

$$k_{ez} = \frac{2\pi D}{\mu_0 \nu} \tag{13}$$

Table 2 gives channel-base current peaks estimated from far vertical electric-field peaks shown in Fig. 4 using Eq. (13), which does not consider the channel inclination. Table 3 gives those estimated using Eq. (12), which considers the channel inclination. It appears from Tables 2 and 3 that Eq. (13) does not allow one to estimate the current peaks for an inclined lightning channel accurately, but Eq. (12) can, provided that the inclination angle  $\alpha$  is given. In the latter case, the error is within 8%. This result is for current risetime of 1  $\mu$ s and it remains essentially the same if the current risetime is changed to 3  $\mu$ s. In Appendix A1, we present similar derivations and analysis for estimation of the peak of channel-base current from the peak of azimuthal magnetic field observed more than some tens of kilometers from an inclined lightning channel.

Fig. 5 shows the ratio of the electric-field peak at a distance of 100 km from the channel base, in the case of a channel with an angle  $\alpha$  (when  $\beta=90^\circ$ ) ranging from -90 to  $90^\circ$ , to the electric-field peak in the case of vertical channel ( $\alpha=0$ ), calculated using Eq. (12). The propagation speed of lightning return-stroke current vary from c/3 to c/2. It follows from Fig. 5 that the influence of channel inclination is slightly larger as the current propagation speed increases.

The angle  $\alpha_{emax}$ , which gives the maximum value of the far electric field, can be obtained by differentiating Eq. (11) with respect to  $\alpha$  on y-z plane (x=0 and  $\beta=90$  degrees) and equating it to 0 ( $\partial E_z/\partial \alpha=0$ ) as follows:

$$\alpha_{\rm emax} = tan^{-1} \left( \frac{v}{\sqrt{c^2 - v^2}} \right) \tag{14}$$

For v=c/3 and v=c/2,  $\alpha_{emax}$  is 22 and 33°, respectively. These results agree well with Fig. 5.

## 5. Expression for estimating channel-base current waveshape from far electric-field waveform

In this section, we derive an expression to estimate the waveform of channel-base current from the waveform of far vertical electric field considering the inclination of lightning channel and the attenuation of current along the channel. The after-the-peak waveform of lightning electric field beyond some tens of kilometers is due to both the induction and radiation components (electrostatic component is negligible). Hence, the expression of the electric field is given as the sum of the radiation and induction components, which is derived from Eq. (1) and Eq. (10) as follows:

$$\begin{split} E_{z}(x, y, t) &\approx E_{zi} + E_{zr} \\ &= \int_{0}^{L_{R}(t)} C_{ezi}(l)I(l, t - R/c)dl - \int_{0}^{L_{R}(t)} C_{ezr}(l) \frac{\partial I(l, t - R/c)}{\partial t} dl \\ &= \int_{0}^{L_{R}(t)} C_{ezi}(l)I(l, t - R/c)dl \\ &- \int_{0}^{L_{R}(t)} C_{ezr}(l)P(l)S(l) \frac{\partial I(t - R/c - l/v)}{\partial l} dl \\ &= \int_{0}^{L_{R}(t)} C_{ezi}P(l)I(t - R/c - l/v)dl \\ &- C_{ezr}(l)P(l)S(l)I(t - R/c - l/v)|_{l=L_{R}(t)} \\ &+ C_{ezr}(0)P(0)S(0)I(t - D/c) \\ &+ \int_{0}^{L_{R}(t)} \frac{\partial}{\partial l} [C_{ezr}(l)P(l)S(l)]I(t - R/c - l/v)dl \\ &= \int_{0}^{L_{R}(t)} \left\{ C_{ezi}(l)P(l) + \frac{\partial}{\partial l} [C_{ezr}(l)P(l)S(l)] \right\} I(t - R/c - l/v)dl \\ &- C_{ezr}(l)P(l)S(l)I(t - R/c - l/v)|_{l=L_{R}(t)} \\ &- \frac{1}{k_{ez}} I(t - D/c) \end{split}$$

From Eq. (15), the channel-base current is expressed as follows:

$$\approx k_{ez} \begin{bmatrix} -E_{z}(x, y, t) \\ + \int_{0}^{L_{R}(t)} \left\{ C_{ezi}(l)P(l) + \frac{\partial}{\partial l} [C_{ezr}(l)P(l)S(l)] \right\} \\ \times I(t - R/c - l/v)dl \\ -C_{ezr}(l)P(l)S(l)I(t - R/c - l/v)|_{l = L_{R}(t)} \end{bmatrix}$$
(16)

Approximating the integral in Eq. (16) by summation yields the following expression:

 $I(n\Delta t) \approx$ 

$$k_{ez} \begin{bmatrix} E_z(n\Delta t + D/c) \\ + \sum_{k=1}^{m} \left\{ C_{ezi}(l)P(l) + \frac{\partial}{\partial l} [C_{ezr}(l)P(l)S(l)] \right\} \\ \times I(k\Delta t - R/c - l/v + D/c)v\Delta t \\ - C_{ezr}(l)P(l)S(l)I(n\Delta t - R/c - l/v + D/c)l_{=L_R(n\Delta t + D/c)} \end{bmatrix}$$

$$(17)$$

where m=n for  $n \le L/(\nu \Delta t)$  and  $m=\lceil L/(\nu \Delta t)\rceil$  for  $n > L/(\nu \Delta t)$ , and  $\Delta t$  is the time step. Note that the time origin of the current is shifted by D/c for adjusting to the channel-base current. Also note that  $\partial [C_{exr}(l)P(l)S(l)]/\partial l$  is obtained using Maplesoft (Bernardin et al. 2020 [39]) (see Appendix A2).

The current waveforms at the channel base calculated using Eq. (17)

from electric field waveforms (including both induction and radiation components) at 100 km are shown in Fig. 6. For comparison, current waveforms calculated considering the radiation component only (all other conditions being the same) are shown in Fig. 7. Table 4 gives the ratio of the channel-base current at 100  $\mu s$  (wavetail), estimated with Eq. (17), to the corresponding actual (original) value. The estimated currents are only about 20 to 30% higher than the actual value. Note that the accuracy for the lightning current with a risetime of 3  $\mu s$  is almost the same, although the results are not shown here.

Table 5 gives the ratio of the channel-base current at 100  $\mu s,$  estimated with an equation considering the radiation component only, to the corresponding actual value. The estimated currents are higher than the actual value by a factor of 1.5 to 2.2. Clearly, the induction field component is not negligible at later times.

## 6. Conclusions

Vertical electric field and azimuthal magnetic field waveforms on flat perfectly conducting ground at a distance of 100 km radiated from an inclined lightning channel were computed using theoretical expressions with three engineering models of the lightning return stroke: the TL, MTLL, and MTLE models. It was shown that the inclination of the lightning channel significantly influences far lightning electric and magnetic field waveforms, and the influence slightly increases with increasing the current propagation speed. Two expressions to estimate the peak of lightning channel-base current or its waveform from the peak of a far vertical electric or azimuthal magnetic field waveform radiated from an inclined lightning channel or its waveform, respectively, were derived. The first expression, derived from the relation between the channel-base current and the radiation field component, allows one to estimate the peak of the channel-base current from a far-

field peak within an 8% error if the channel inclination angle is known (usually from optical observations). The second expression, derived from the relation between the channel-base current and both induction and radiation field components, can reconstruct sufficiently accurately the waveform of channel-base current from the field waveform, again if the channel inclination angle is known.

## CRediT authorship contribution statement

K. Kutsuna: Conceptualization, Methodology, Software, Investigation, Writing – original draft. N. Nagaoka: Supervision, Investigation, Writing – review & editing. Y. Baba: Supervision, Investigation, Writing – review & editing. T. Tsuboi: Writing – review & editing. V.A. Rakov: Supervision, Writing – review & editing.

## **Declaration of Competing Interest**

The authors declare that they have no known competing financial interests or personal relationships that could have appeared to influence the work reported in this paper.

## Data availability

The data that has been used is confidential.

#### Acknowledgement

This work was supported in part by the U.S. National Science Foundation under grant AGS-2055178.

## **Appendix**

#### A1. Expression for Estimating Channel-Base-Current Waveform from Far Magnetic-Field Waveform

In this appendix, an expression to estimate the channel-base-current waveform from the far azimuthal magnetic-field waveform for an inclined lightning channel is derived, and its validity is examined. The azimuthal magnetic field  $H_{\varphi}$  at the observation point (x, y) on a perfectly conducting ground associated with a current wave I propagating along an inclined lightning channel, as shown in Fig. 1, is given as follows [23,24]:

$$H_{\varphi}(x, y, t) = H_{\varphi i} + H_{\varphi r}$$

$$= \int_{0}^{L_{R}(t)} C_{h\varphi i}(l) I(l, t - R/c) dt$$

$$+ \int_{0}^{L_{R}(t)} C_{h\varphi r}(l) \frac{\partial I(l, t - R/c)}{\partial t} dl$$

$$(18)$$

where

$$\begin{cases} C_{h\varphi i}(l) = \frac{D\cos\alpha}{2\pi R^3} \\ C_{h\varphi r}(l) = \frac{D\cos\alpha}{2\pi cR^2} \\ l = \sqrt{x'^2 + y'^2 + z'^2} \end{cases}$$

$$(19)$$

The initial peak of lightning electromagnetic field beyond some tens of kilometers is essentially due to the contribution of the radiation component. The radiation component of the azimuthal magnetic field, given as the second term of the right-hand side of Eq. (18), is rewritten as follows:

$$(20)$$

$$= \int_{0}^{L_{R}(t)} C_{h\varphi r}(t) P(t) \frac{\partial I(t, t - R/c)}{\partial t} dt$$

$$\approx \frac{v \cos \alpha}{2\pi [cD - v \sin \alpha (x \cos \beta + y \sin \beta)]} I(t - D/c)$$

where P(l) is the current attenuation function, which is 1, (1-l/L), and exp  $(-l/\lambda)$  for the TL, MTLE, and MTLE models, respectively. Therefore, the channel-base current peak  $I_{peak}$  is estimated from the peak of the azimuthal magnetic field  $H_{dpeak}$  at a far distance as follows:

$$I_{peak} \approx k_{h\varphi} H_{\phi peak}$$

$$k_{h\varphi} = \frac{2\pi [cD - v\sin\alpha(x\cos\beta + y\sin\beta)]}{v\cos\alpha}$$
(21)

where  $k_{h\varphi}$  is a magnetic-field-to-current conversion factor. For a vertical lightning channel ( $\alpha = 0$ ),  $k_{h\varphi}$  is given simply as follows:

$$k_{h\varphi} = \frac{2\pi cD}{v} \tag{22}$$

The angle  $\alpha_{hmax}$ , which gives the maximum value of the far magnetic field, is obtained by differentiating Eq. (20) with respect to  $\alpha$  on y-z plane (x = 0 and  $\beta$  = 90 degrees) and equating it to 0 ( $\partial H_{\omega}/\partial \alpha$  = 0). It is the same as Eq. (14).

Fig. 8 shows waveforms of the azimuthal magnetic field at a distance of D = 100 km from the base of an inclined lightning channel computed with the TL, MTLL, and MTLE models for different inclination angles,  $\alpha = -60$ , -30, 0 (vertical channel), +30 and +60°. The waveforms of lightning channel

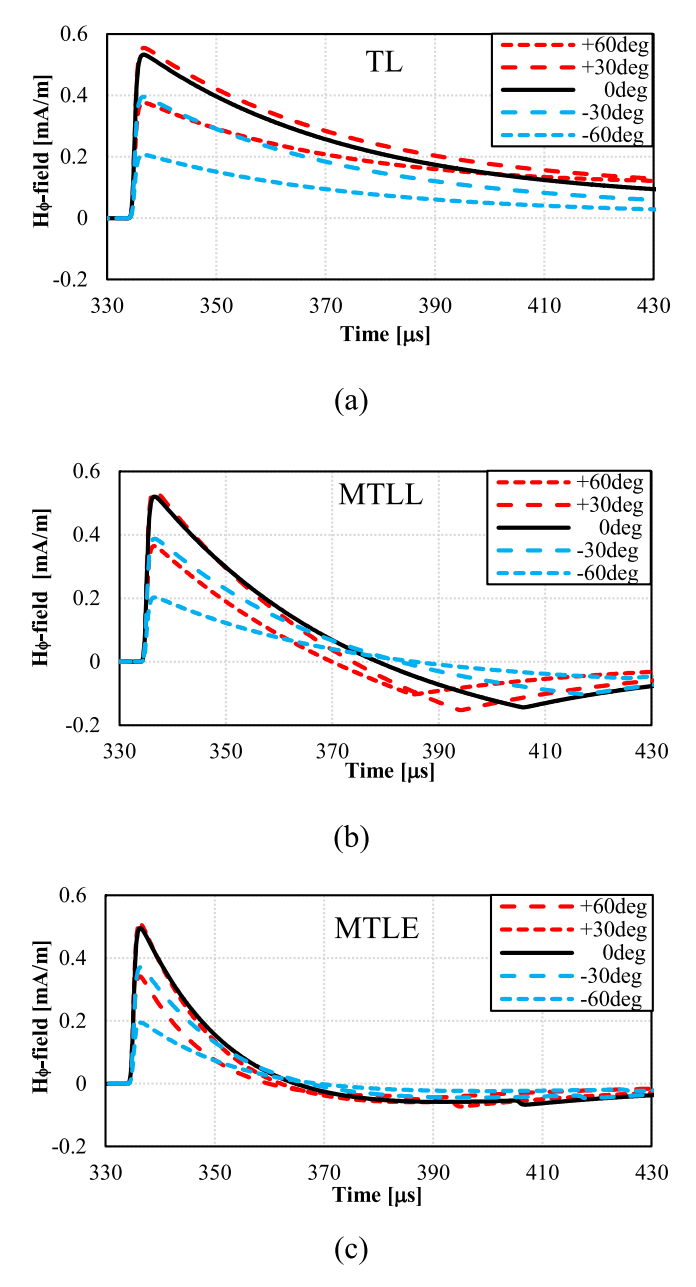


**Fig. 8.** Azimuthal magnetic field waveforms for unit-peak channel-base current waveform at a distance of 100 km from the base of an inclined lightning channel computed with (a) the TL model, (b) the MTLL model, and (c) the MTLE model (see Fig. 2) for different inclination angles:  $\alpha = -60$ , -30, 0, +30 and +60 deg (RT = 1  $\mu$ s, v = c/3).

Table 6
Peaks of azimuthal magnetic field waveforms for unit-peak current waveforms at a distance of 100 km from the base of the inclined lightning channel. Units [mA/m].

| Model | Inclination angle of l | ightning channel $\alpha$ |       |         |         |
|-------|------------------------|---------------------------|-------|---------|---------|
|       | -60 deg                | -30 deg                   | 0 deg | +30 deg | +60 deg |
| TL    | 0.21                   | 0.40                      | 0.53  | 0.55    | 0.38    |
| MTLL  | 0.20                   | 0.39                      | 0.52  | 0.54    | 0.36    |
| MTLE  | 0.19                   | 0.37                      | 0.50  | 0.51    | 0.34    |

Table 7
Channel-base-current peaks (in kA) estimated from far azimuthal magnetic field peaks without considering channel inclination. The actual current peak is 1 kA.

| Model | Inclination angle of l | ightning channel $\alpha$ |       |         |         |  |  |
|-------|------------------------|---------------------------|-------|---------|---------|--|--|
|       | -60 deg                | -30 deg                   | 0 deg | +30 deg | +60 deg |  |  |
| TL    | 0.39                   | 0.74                      | 1.0   | 1.0     | 0.71    |  |  |
| MTLL  | 0.38                   | 0.73                      | 0.98  | 1.0     | 0.69    |  |  |
| MTLE  | 0.37                   | 0.70                      | 0.93  | 0.96    | 0.64    |  |  |

Table 8
Channel-base-current peaks (in kA) estimated from far azimuthal magnetic field peaks considering channel inclination. The actual current peak is 1 kA.

| Model | Inclination angle of l | ightning channel $\alpha$ |       |         |         |
|-------|------------------------|---------------------------|-------|---------|---------|
|       | -60 deg                | -30 deg                   | 0 deg | +30 deg | +60 deg |
| TL    | 1.0                    | 1.0                       | 1.0   | 1.0     | 1.0     |
| MTLL  | 0.98                   | 0.98                      | 0.98  | 0.98    | 0.98    |
| MTLE  | 0.95                   | 0.94                      | 0.93  | 0.93    | 0.92    |

current are shown in Fig. 2. The risetime of current is 1  $\mu$ s, and the current propagation speed is set to v = c/3. Table 6 gives the peaks of the azimuthal magnetic field. It appears from Fig. 8 and Table 6 that azimuthal magnetic fields at D = 100 km are significantly influenced by channel inclination. Table 7 gives channel-base current peaks estimated from far azimuthal magnetic-field peaks shown in Fig. 8 using Eq. (22), which does not consider the channel inclination. Table 8 gives those estimated using Eq. (21), which considers the channel inclination.

It appears from Tables 7 and 8 that Eq. (22) cannot estimate the current peaks for inclined lightning channel accurately but Eq. (21) can do reasonably accurately if the inclination angle  $\alpha$  is given.

The expression for estimating the channel-base-current waveform from a far azimuthal-magnetic-field waveform is derived from both induction and radiation components of Eq. (18) in the same manner as done for vertical electric field, Eq. (17). It is given as follows:

$$I(n\Delta t) =$$

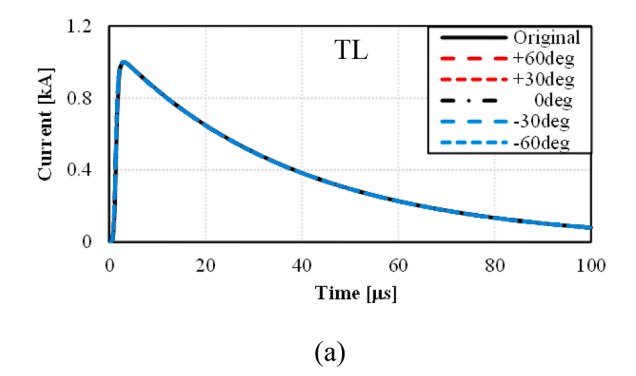
$$k_{h\phi} \begin{bmatrix} H_{\phi}(n\Delta t + D/c) \\ -\sum_{k=1}^{m} \left\{ C_{h\phi i} P(l) + \frac{\partial}{\partial l} \left( C_{h\phi r} P(l) S(l) \right) \right\} \\ \times I(k\Delta t - R/c - l/v + D/c) v \Delta t \\ -C_{h\phi r} P(l) S(l) I(n\Delta t - R/c - l/v + D/c) |_{l=L_{R}(n\Delta t + D/c)} \end{bmatrix}$$

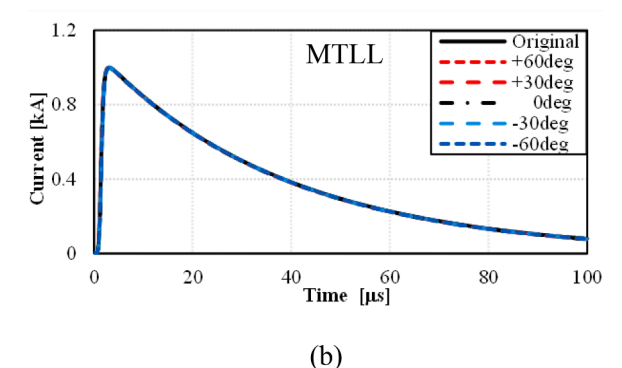
$$(23)$$

where m = n for  $n \le L/(v\Delta t)$  and  $m = \lceil L/(v\Delta t) \rceil$  for  $n > L/(v\Delta t)$ ,  $\Delta t$  is the time step. The current waveforms at the channel base calculated using Eq. (23) from far electric-field waveforms are shown in Fig. 9. It follows from Fig. 9 that Eq. (23) reasonably accurately reproduces the waveform of channel-base current from the corresponding waveform of azimuthal magnetic field at a distance of 100 km, regardless of channel inclination.

## A2. Derivative Expressions Given by Maplesoft

In this appendix, we give expressions for  $\partial [C_{ezr}(l)P(l)S(l)]/\partial l$  in Eq. (17), obtained using Maplesoft [39] for the TL, MTLL, and MTLE models (see Eqs. (24), (25), and (26), respectively). The partial derivative for each of the models is expressed as a ratio of two functions whose numerator and denominator are listed below, with expressions for  $C_{ezr}(l)$ , P(l), and S(l) being found in Eqs. (2), (7), and (8), respectively.





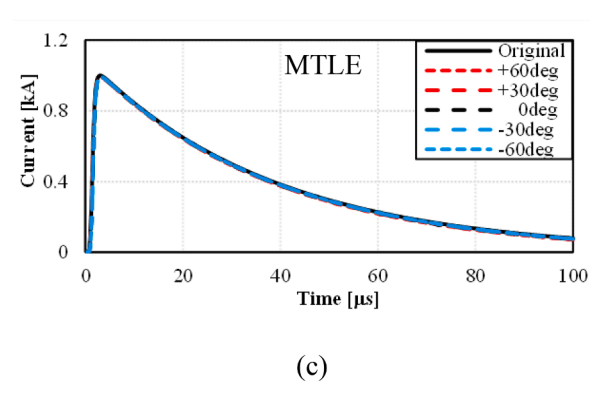


**Fig. 9.** Waveforms of channel-base current estimated from azimuthal magnetic-field waveforms (both induction and radiation field components are taken into account) at a distance of 100 km from the inclined lightning channel with (a) the TL model, (b) the MTLL model, and (c) the MTLE model for different inclination angles:  $\alpha = -60$ , -30, 0, +30 and +60 deg ( $RT = 1 \mu s$ , v = c/3). Additionally shown by solid black line is the original channel-base current waveform, which is indistinguishable from the current waveforms estimated from field waveforms.

Numerator of  $\frac{\partial}{\partial l}[C_{exr}(l)P(l)S(l)]$  for the TL model :

$$-y\cos\alpha \begin{cases} v\sqrt{t^2 - 2ly\sin\alpha + y^2} \begin{bmatrix} (l^2 + y^2(3 - \cos^2\alpha))l\sin\alpha \\ +\frac{3}{2}y\left((l^2 + y^2)\cos^2\alpha - 2l^2 - \frac{2y^2}{3}\right) \end{bmatrix} \\ +c \begin{bmatrix} (t^4 + l^2y^2(6 - \cos^2\alpha) + y^4)\sin\alpha \\ +\frac{5}{2}ly(l^2 + y^2)\left(\cos^2\alpha - \frac{8}{5}\right) \end{bmatrix} \end{cases}$$

Denominator of  $\frac{\partial}{\partial l}[C_{ezr}(l)P(l)S(l)]$  for the TL model :

$$\pi \varepsilon_0 v c^3 \sqrt{l^2 - 2ly \sin\alpha + y^2} \left\{ \begin{bmatrix} -6ly(l^4 + y^4) + l^3 y^3 (8\cos^2\alpha - 20) \end{bmatrix} \sin\alpha \\ + (l^2 + y^2) [l^4 + (14 - 12\cos^2\alpha)l^2 y^2 + y^4] \right\}$$
(24)

Numerator of  $\frac{\partial}{\partial l}[C_{ezr}(l)P(l)S(l)]$  for the MTLL model:

$$= \int_{v\sqrt{l^2 - 2ly\sin\alpha + y^2}} \left[ \sin\alpha \left[ (3 - \cos^2\alpha)Ly^2 l + \frac{y^4}{2} + l^3 \left( L - \frac{l}{2} \right) \right] \right]$$

$$= -y\cos\alpha \left\{ -y\cos\alpha \left\{ -\frac{l^2y^2 (l + L)\cos^2\alpha + \left( L + \frac{3l}{2} \right)y^4 \right\} \sin\alpha + \left( (6Ll^2 - l^3)y^2 + l^4 \left( -\frac{l}{2} + L \right) \right) \sin\alpha + \left( (1 + \frac{5}{2}y^4 + \frac{1}{2}y^4 + \frac{1}{2}y^2 + \frac{1}{2}y^4 + \frac{1}{2}y^2 + \frac{1}{2}y^4 + \frac{1}{2}y^2 + \frac{1$$

Denominator of  $\frac{\partial}{\partial l}[C_{ezr}(l)P(l)S(l)]$  for the MTLL model:

$$\begin{bmatrix}
-6\pi\varepsilon_{0}vc^{3}L\sqrt{l^{2}-2ly\sin\alpha+y^{2}} & \left[l^{4}+\frac{10-4\cos^{2}\alpha}{3}l^{2}y^{2}+y^{4}\right]ly\sin\alpha \\
-\frac{(l^{2}+y^{2})\left[(14-12\cos^{2}\alpha)l^{2}y^{2}+l^{4}+y^{4}\right]}{6}\right]
\end{cases}$$
(25)

Numerator of 
$$\frac{\partial}{\partial l}[C_{ezr}(l)P(l)S(l)]$$
 for the MTLE model :

$$\begin{cases} v\sqrt{l^{2}-2ly\sin\alpha+y^{2}} \begin{bmatrix} \left(-2ly^{2}(l+\lambda)\cos^{2}\alpha+y^{4}\right)\sin\alpha\\ +6ly^{2}(l+\lambda)+l^{3}(l+2\lambda) \end{pmatrix} \sin\alpha\\ +y\sqrt{l^{2}-2ly\sin\alpha+y^{2}} \begin{bmatrix} \left(-2ly^{2}(l+\lambda)\cos^{2}\alpha+y^{4}\right)\sin\alpha\\ +y\sqrt{l^{2}-2l^{2}(2l+\lambda)+l^{3}(l+2\lambda)} \end{bmatrix} \\ +\sqrt{l^{2}-2ly\sin\alpha+y^{2}} \begin{bmatrix} \left(-2y^{2}l^{2}\cos^{2}\alpha(2l+\lambda)+(5l+2\lambda)y^{4}\right)\sin\alpha\\ +(10l+12\lambda)l^{2}y^{2}+(l+2\lambda)l^{4} \end{bmatrix} \sin\alpha\\ +c \begin{bmatrix} \left(\left(2l+\frac{5}{4}\lambda\right)y^{2}+\left(l+\frac{5}{4}\lambda\right)l^{2}\right)l\cos^{2}\alpha\\ -\frac{y^{4}}{4}+\left(-2\lambda l-\frac{5}{2}l^{2}\right)y^{2}-2l^{3}\lambda-\frac{5}{4}l^{4} \end{bmatrix} \end{bmatrix}$$

Denominator of  $\frac{\partial}{\partial l}[C_{ex}(l)P(l)S(l)]$  for the MTLE model :

$$\left\{ \pi \epsilon_0 \lambda v c^3 \sqrt{t^2 - 2ly \sin\alpha + y^2} \begin{cases} \left[ y^2 t^2 \left( 10 - 4 \cos^2 \alpha \right) \right] 4 ly \sin\alpha \\ + 3 \left( t^4 + y^4 \right) \right] 4 ly \sin\alpha \\ - 2 \left( t^2 + y^2 \right) \left[ t^4 + y^4 \\ + \left( 14 - 12 \cos^2 \alpha \right) t^2 y^2 \right] \end{cases} \right\}$$

## References

- [1] V. Kodali, V.A. Rakov, M..A. Uman, K.J. Rambo, G.H. Schnetzer, J. Schoene, J. Jerauld, Triggered-lightning properties inferred from measured currents and very close electric fields, Atmos Res. 76 (1–4) (2005) 355–376, https://doi.org/ 10.1016/j.atmosres.2004.11.036.
- [2] X. Qie, Y. Zhao, Q. Zhang, J. Yang, G. Feng, X. Kong, Y. Zhou, T. Zhang, G. Zhang, T. Zhang, D. Wang, H. Cui, Z. Zhao, S. Wu, Characteristics of triggered lightning during Shandong artificial triggering lightning experiment (SHATLE), Atmos Res. 91 (2–4) (2009) 310–315, https://doi.org/10.1016/j.atmosres.2008.08.007.
- [3] H. Norinder, O. Dahle, Measurements by frame aerials of current variations in lightning discharges, Arkiv. Mat. Astron. Fysik (32A) (1945) 1–70.
- [4] M.A. Uman, D.K. McLain, Lightning return stroke current from magnetic and radiation field measurements, J. Geophys. Res. 75 (27) (1970) 5143–5147, https:// doi.org/10.1029/JC075i027p05143.
- [5] M.A. Uman, D.K. McLain, R.J. Fisher, E.P. Krider, Electric field intensity of the lightning return stroke, J. Geophys. Res. 78 (18) (1973) 3523–3529, https://doi. org/10.1029/JC078i018p03523.
- [6] M.A. Uman, D.K. McLain, R.J. Fisher, E.P. Krider, Currents in Florida lightning return strokes, J. Geophys. Res. 78 (18) (1973) 3530–3537, https://doi.org/ 10.1029/JC078i018n03530.
- [7] A.A. Dulzon, V.A. Rakov, Estimation of errors in lightning peak current measurements by frame aerials, Izv. VUZov SSSR, ser. Energetika 11 (1980) 101–104.
- [8] E.P. Krider, C. Leteinturier, J.C. Willett, Submicrosecond fields radiated during the onset of first return strokes in cloud-to-ground lightning, J. Geophys. Res. 101 (D1) (1996) 1589–1597, https://doi.org/10.1029/95JD02998.
- [9] K.L. Cummins, E.P. Krider, M.D. Malone, The US National Lightning Detection Network™ and applications of cloud-to-ground lightning data by electric power utilities, IEEE Trans. Electromagn. Compat. 40 (4) (1998) 465–480, https://doi. org/10.1109/15.736207.
- [10] F. Rachidi, J.L. Bermudez, M. Rubinstein, V.A. Rakov, On the estimation of lightning peak currents from measured fields using lightning location systems, J. Electrostatics 60 (2–4) (2004) 121–129, https://doi.org/10.1016/j. elstat.2004.01.010.
- [11] S. Mallick, V.A. Rakov, D. Tsalikis, A. Nag, C. Biagi, D. Hill, D.M. Jordan, M. A. Uman, J.A. Cramer, On remote measurements of lightning return stroke peak currents, Atmos Res. 135–136 (2014) 306–313, https://doi.org/10.1016/j.atmosres.2012.08.008.
- [12] F. Rachidi, R. Thottappillil, Determination of lightning currents from far electromagnetic fields, J. Geophys. Res. 98 (D10) (1993), 18,315-18,321, Oct.

- [13] C.E.R. Bruce, R.H. Golde, The lightning discharge, J. Institution of Electr. Eng. 88 (1941) 487–520.
- [14] M.A. Uman, D.K. McLain, Magnetic field of the lightning return stroke, J. Geophys. Res. 74 (1969), 6,899-6,910.
- [15] C.A. Nucci, C. Mazzetti, F. Rachidi, M. Ianoz, On lightning return stroke models for LEMP calculation, in: Paper presented at the 19th Int. Conf. Lightning Protection, Graz, Austria, 1988, pp. 463–470.
- [16] M.J. Master, M.A. Uman, Y.T. Lin, R.B. Standler, Calculations of lightning return stroke electric and magnetic fields above ground, J. Geophys. Res. 86 (1981), 12,127-12,132.
- [17] F. Heidler, Traveling current source model for LEMP calculation, in: Paper presented at the Int. Symp. EMC, Zurich, no. 29F2, 1985, pp. 157–162.
- [18] G. Diendorfer, M.A. Uman, An improved return stroke model with specified channel base current, J. Geophys. Res. 95 (1990), 13,621-13,644.
- [19] V.A. Rakov, A.A. Dulzon, Calculated electromagnetic fields of lightning return stroke" (in Russian), Tekhnicheskaya Elektrodinamika 1 (1987) 87–89.
- [20] A. Andreotti, U. De Martinis, L. Verolino, A method for the identification of the return stroke model, in: Paper presented at the 25th International Conference on Lightning Protection, Rhodes, Greece, 2000, pp. 113–117. Sep.
- [21] M. Popov, S. He, R. Thottappillil, Reconstruction of lightning currents and return stroke model parameters using remote electromagnetic fields, J. Geophys. Res. 105 (D19) (2000), 24,469-24,481, Oct.
- [22] M. Fukuyama, S. Koike, Y. Baba, T. Tsuboi, V.A. Rakov, Reconstruction of channel-base-current waveforms from electromagnetic field waveforms degraded by propagation effects, in: International Conference on Lightning Protection/International Symposium on Lightning Protection (ICLP-SIPDA), no. 230, Sri Lanka (Virtual Conference), 2021. Sep.
- [23] Adel Z. El Dein, G. Shabib, Said I. Abouzeid, New electromagnetic expressions due to inclined lightnig channel, in: 16th International Middle-East Power Conference, Egypt, Ain Shams University, 2014. Dec.
- [24] Said I. Abouzeid, G. Shabib, Adel Z.El Dein, Analysis of electromagnetic fields generated by inclined lightning channel, Arabian J. Sci. Eng. 40 (2015) 2555-2608
- [25] A. Sakakibara, Calculation of induced voltages on overhead lines caused by inclined lightning strokes, IEEE Trans. Power Del. 4 (1) (1989) 68–693. Jan.
- [26] K. Michishita, M. Ishii, Y. Hongo, Induced voltage on an overhead wire associated with inclined return-stroke channel-model experiment on finitely conductive ground, IEEE Trans. Electromag. Compat. 38 (3) (1996) 507–513. Aug.
- [27] R. Moini, S.H. Sadeghi, B. Kordi, F. Rachidi, An antenna-theory approach for modeling inclined lightning return stroke channels, Electr. Power Syst. Res. 76 (11) (2006) 945–952. Jul.

(26)

- [28] I. Matsubara, S. Sekioka, Analytical formulas for induced surges on a long overhead line caused by lightning with an arbitrary channel inclination, IEEE Trans. Electromagn. Compat. 51 (3) (2009) 733–740. Aug.
- [29] A. Andreotti, C. Petrarca, V.A. Rakov, L. Verolino, Calculation of voltages induced on overhead conductors by nonvertical lightning channels, IEEE Trans. Electromagn. Compat. 54 (4) (2012) 860–870. Aug.
- [30] A. Foroughi Nematollahi, B. Vahidi, 3D FEM analysis of induced current in the shield of the buried cable by non-vertical channel, Electr. Power Syst. Res. 212 (2022), https://doi.org/10.1016/j.epsr.2022.108256. Nov.
- [31] V.A. Rakov, Lightning return stroke speed, J. Lightning Res. 1 (2007) 80-89.
- [32] F. Heidler, Analytical lightning current function for LEMP-calculation, in: International Conference on Lightning Protection, Munich/Germany, 1985, pp. 63–66.
- [33] C.A. Nucci, G. Diendorfer, M.A. Uman, F. Rachidi, M. Ianoz, C. Mazzetti, Lightning return stroke current models with specified channel-base current: a review and comparison, J. Geophys. Res. 95 (D12) (1990) 20395–20408. Nov.

- [34] V.A. Rakov, M.A. Uman, Review and evaluation of lightning return stroke models including some aspects of their application, IEEE Trans. Electromagn. Compat. 40 (4) (1998) 403–426. Nov.
- [35] P. Hubert, G. Mouget, Return stroke velocity measurements in two triggered lightning flashes, J. Geophys. Res. 86 (C6) (1981) 5253–52661.
- [36] V.P. Idone, R.E. Orville, P. Hubert, L. Barret, A. Eybert-Berard, Correlated observations of three triggered lightning flashes, J. Geophys. Res. 89 (D1) (1984) 1385–1394.
- [37] J.C. Willett, D.M. Le Vine, V.P. Idone, Lightning return stroke current waveforms aloft from measured field change, current, and channel geometry, J. Geophys. Res. 113 (D07305) (2008), https://doi.org/10.1029/2006JD008116.
- [38] W. Lu, Y. Gao, L. Chen, Q. Qi, Y. Ma, Y. Zhang, S. Chen, X. Yan, C. Chen, Y. Zhang, Three-dimensional propagation characteristics of the leaders in the attachment process of a downward negative lightning flash, J. Atmospheric and Solar-Terrestrial Phys. 136 (2015), https://doi.org/10.1016/j.jastp.2015.07.011.
- [39] L. Bernardin, P. Chin, P. DeMarco, K.O. Geddes, D.E.G. Hare, K.M. Heal, G. Labahn, J.P. May, J. McCarron, M.B. Monagan, D. Ohashi, S.M. Vorkoetter, Maple Programming Guide, Maplesoft, Waterloo Maple Inc., Waterloo, Canada, 2020.